JOURNAL OF MAGNETIC RESONANCE **38,** 453–479 (1980)

Radiofrequency Pulse Sequences Which Compensate Their Own Imperfections*

RAY FREEMAN, STEWART P. KEMPSELL, AND MALCOLM H. LEVITT

Physical Chemistry Laboratory, Oxford, England

Received September 13, 1979

Radiofrequency pulse sequences are described which have the same overall effect as a single 90 or 180° pulse but which compensate the undesirable effects of resonance offset and spatial inhomogeneity of the radiofrequency field H_1. These "composite" pulses are built up from a small number of conventional pulses which rotate the nuclear magnetization vectors about different axes in the rotating frame, while in the intervals between pulses a limited amount of free precession may be allowed to occur. Insight into the way in which pulse imperfections are compensated is obtained by computer simulation of trajectories of families of nuclear spin "isochromats" representing a distribution of H_1 intensity or resonance offset. Composite 90° pulses are suggested as a method of reducing systematic errors in spin–lattice relaxation times derived from progressive saturation or saturation–recovery experiments, and as the preparation pulse of a spin-locking experiment. A test of the effectiveness of the composite 180° pulse sequence has been made by using it for population inversion in a spin–lattice relaxation measurement where T_1 is derived from the null point in the recovery curve, a technique known to be very sensitive to pulse imperfections.

INTRODUCTION

Pulse excitation has now become an essential part of high-resolution NMR, both for routine operation and for more sophisticated experiments to study relaxation, chemical exchange, multiple-quantum transitions, and two-dimensional Fourier transform spectra. Pulse imperfections therefore merit a closer study, and this work suggests methods for compensating such imperfections by replacing each radiofrequency pulse by a composite pulse—a cluster of closely spaced pulses which achieves the same nominal flip angle, but which has a higher tolerance of the most common imperfections, spatial inhomogeneity of the radiofrequency field and resonance offset effects.

The intensity of the radiofrequency field H_1 varies in different geometrical regions of the sample, normally having the highest intensity near the center of the transmitter coils and falling off in regions remote from the center. This spatial inhomogeneity of H_1 introduces serious errors in the flip angle $\gamma H_1 t_p$ experienced by the nuclei in different volume elements. Attempts to circumvent the problem, by using small bulb samples rather than long cylindrical samples, suffer from poor sensitivity and often

* First presented at the 20th Experimental NMR Conference, Asilomar, Calif., February 1979.

0022-2364/80/060453-27$02.00/0

DOI of original item: doi: 10.1016/0022-2364(80)90327-3

have difficulties with distortion of the static field H_0 by discontinuities in magnetic susceptibility.

The second type of pulse imperfection arises because H_1 has a finite intensity compared with typical offsets from resonance ΔH. Hence the magnetization vectors rotate about a resultant field H_{eff} which is tilted in the rotating frame. Technological improvements which increase H_1 tend to be matched by developments which increase the applied static field H_0 and hence the chemical shift range. Although quadrature phase detection effectively halves the maximum value of ΔH by allowing the transmitter frequency to be set in the center of the spectrum, resonance offset effects are still a serious problem.

It is proposed to compensate these two kinds of pulse imperfection by replacing the conventional 90 or 180° pulse by a corresponding composite pulse. This is defined here as a sequence of two or more radiofrequency pulses separated by intervals so short that no significant relaxation occurs, and any free precession between pulses is usually of the order of 1 radian or less. In certain sequences this precessional motion is essential to the process of compensation; in others free precession is simply minimized and neglected. It is important to note the assumption, made throughout these calculations, that the initial condition of the nuclear magnetization vector is longitudinal, often the equilibrium magnetization M_0 aligned along $+Z$. This excludes the case of 180° pulses used for refocusing isochromats in the XY plane, as in the Carr–Purcell spin-echo experiment (*1*).

The motion of the nuclear magnetization subjected to a composite pulse may be described by the Bloch equations neglecting relaxation. Figure 1 shows the rotating

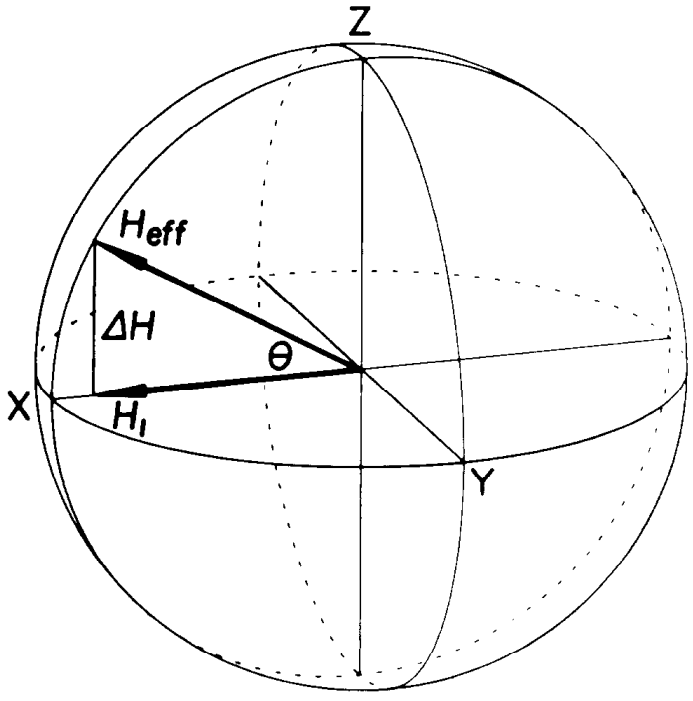

FIG. 1. The effective field operating on nuclear spin magnetization vectors, viewed in a reference frame rotating in synchronism with the transmitter frequency.

frame employed, with H_1 a static vector aligned along the X axis, and the effective field H_{eff} tilted with respect to H_1 through θ in the XZ plane.

$$H_{\text{eff}} = (H_1^2 + \Delta H^2)^{1/2}, \quad [1]$$

$$\tan\theta = \Delta H / H_1. \quad [2]$$

The mechanism by which pulse imperfections are compensated may be visualized by following a family of spin "isochromats" representing either a distribution of values of H_1 or a distribution of values of the resonance offset ΔH. These isochromats are represented by vectors which alternately rotate about H_{eff} during the pulses and precess about the offset field ΔH in the interval between pulses. Although the overall effect of the composite pulse sequence is the solution of a simple problem in spherical geometry, the analytical solution is often complex and uninformative. Therefore the treatment which follows makes extensive use of computer simulation, which readily handles sequences of several pulses and which allows greater insight into the principles involved.

For NMR lines sufficiently close to resonance that $H_1 \gg \Delta H$, a radiofrequency pulse of duration t_p and intensity H_1 nutates the nuclear magnetization through $\gamma H_1 t_p$ radians about the X axis of the rotating frame. In practical cases there is a distribution of values of H_1 in different regions of the sample. In order to be able to describe the various pulses, it is convenient to introduce a nominal value of the radiofrequency field, H_1°, that is representative of the actual intensities near the central region of the transmitter coils. (These regions tend to have the highest intensity H_1 and also the strongest coupling of the NMR signal back to the receiver coil.) A convenient definition of H_1° makes use of a common method of adjusting pulsewidth—searching for the condition $t_{2\pi}$ where the total NMR signal (a weighted average over all sample regions) goes through a null after one complete revolution,

$$\gamma H_1^\circ t_{2\pi} = 2\pi \text{ radians}. \quad [3]$$

(Typical magnetization vectors, of course, nutate through somewhat different angles because of the inhomogeneity of H_1.)

This definition makes it possible to refer to the nominal value of pulse flip angles; for example, a "180° pulse" has $\gamma H_1^\circ t_p = \pi$ radians. In what follows, the quotation marks will be dispensed with, and the terms 90° pulse and 180° pulse will be understood to refer to the nominal value H_1°. Since in practice it is difficult to probe the effects of spatial inhomogeneity of the radiofrequency field directly, some of the experiments to be described use a missetting of t_p to achieve the equivalent of a missetting of H_1.

When the resonance offset ΔH is too large to be neglected in comparison with H_1, then the nuclear magnetization vector nutates through an angle $\gamma H_{\text{eff}} t_p$ radians about an axis which is tilted through θ radians with respect to the XY plane of the rotating frame (Fig. 1). Equation [1] shows that this flip angle will always be greater than that in the on-resonance case. However, it is still convenient to retain the terms "90° pulse" and "180° pulse" on the understanding that they refer to the ideal pulse condition, and that offset and inhomogeneity are simply deviations from the ideal, and indeed are largely compensated by the proposed composite sequences.

In practice both kinds of imperfection operate together and must be treated simultaneously in certain applications. Strictly speaking, this would require a knowledge of the way in which static field inhomogeneities and radiofrequency field inhomogeneities correlate in space. The nature of this correlation is specific to each spectrometer, but fortunately its effect is very small when ΔH is large compared with the instrumental linewidth, and hence it is neglected in all that follows.

In examining the various proposals for composite pulse sequences it is important to clarify whether the compensation acts on radiofrequency inhomogeneity or resonance offset effects, or on both together. Not all the applications require the correction of both types of imperfection.

COMPOSITE 90° PULSES

Compensation for Spatial Inhomogeneity

A conventional 90° pulse, nutating the nuclear magnetization vector about the X axis of the rotating frame, would leave many "isochromats" with finite Z components after the pulse because of the inhomogeneity of the radiofrequency field. Since the pulse length is normally calibrated by observing the aggregate NMR signal, made up principally from sample regions inside the transmitter coil, vectors representing more remote sample regions will show positive Z components of magnetization at the end of the pulse. This can be a source of error in the measurement of spin–lattice relaxation times by the saturation–recovery (*2*) or progressive saturation (*3*) methods. It will be shown that a composite 90° pulse can compensate a significant fraction of these errors. For the purposes of this section, off-resonance effects are neglected.

The proposed sequence is $90°(X)\ 90°(Y)$, nutation through 90° about the X axis followed by nutation through 90° about the Y axis, with the interpulse interval kept as short as possible so that negligible free precession takes place. This notation refers to the nominal values of the pulse length, and any variation in flip angle due to spatial inhomogeneity is of course taken to affect all pulses in exactly the same way. Consider a small volume element of the sample which experiences only 80° pulses. There is a residual Z component after the first pulse of $+M_0 \cos 80°$, but a large proportion of this is removed by the 80° rotation about the Y axis. In effect the error in the Z component has been converted into a corresponding phase error with respect to the Y axis, an admixture of dispersion mode.

Errors arising from radiofrequency inhomogeneity are mainly of concern in spin–lattice relaxation experiments carried out by saturation–recovery or progressive saturation methods. The problem is to ensure that *for each volume element of the sample* M_z after the pulse is as close to zero as possible, even though H_1 is different in different sample regions; it is not sufficient to set the overall Z magnetization to zero. An experimental test of the compensation achieved by the composite 90° pulse was therefore made by monitoring the residual Z magnetization immediately after the composite sequence. This determination was made with the sequence

$$P_1\text{–}t\text{–}P_2\text{–Acq.} \qquad (t > T_2^*),$$

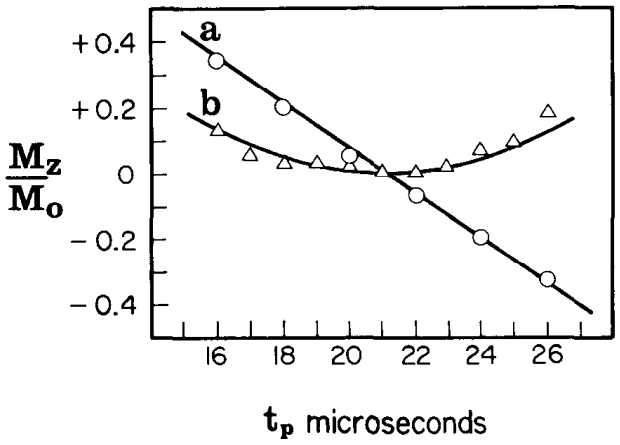

FIG. 2. The residual Z magnetization remaining after (a) a conventional 90°(X) pulse, (b) a composite 90°(X), 90°(Y) pulse. The quantity M_Z is expressed as a fraction of the total equilibrium magnetization M_0. In order to simulate the effect of spatial inhomogeneity in H_1 the pulsewidths t_p have been varied above and below the nominal value (~21 μsec). Note that M_Z after the composite sequence is less sensitive to variation of t_p. The full lines represent calculations based on magnetization trajectories.

where P_2 was in all cases a single "read" pulse with $\gamma H_1^\circ t_p = \pi/2$ radians and P_1 was either a conventional single pulse of flip angle α or a composite $\alpha(X)$, $\alpha(Y)$ sequence where α was varied by varying t_p in order to simulate the effect of spatial inhomogeneity in H_1. The observed signal intensity was plotted as a function of t and extrapolated back to $t = 0$. In order to minimize real radiofrequency inhomogeneity effects, a small spherical bulb sample was used.

When P_1 was a conventional single pulse, the residual Z magnetization showed a strong dependence on pulsewidth t_p, passing through zero near $t_p = 21$ μsec, the condition for $\gamma H_1^\circ t_p = \pi/2$ radians. When P_1 was a composite pulse the Z magnetization went through a shallow minimum as t_p was varied. The experimental points fit very well to the theoretical curves based on simulated magnetization vector trajectories (Fig. 2). It may be inferred from these results that errors in measurements of relaxation times caused by spatial inhomogeneity of the radiofrequency field H_1 should be considerably less serious when a composite sequence is used for saturation.

The compensating effect of the composite 90° pulse can be readily illustrated by computer simulation of trajectories in the rotating frame. In practice the spatial distribution of H_1 intensity is such that volume elements near the center of the transmitter coils have the highest intensity and H_1 falls off for more remote regions of the sample. It is therefore important to compensate for *low* values of H_1, whereas *high* values can normally be neglected. With this kind of distribution a slightly better compensation can be achieved by increasing the flip angle of the second pulse, for example, 90°(X), 110°(Y). Figure 3 illustrates the trajectories of a family of "isochromats" for the 90°(X), 110°(Y) sequence. Note that when the H_1 field intensity is in the range 0.8 to 1.0 H_1°, the trajectories terminate very close to the XY plane.

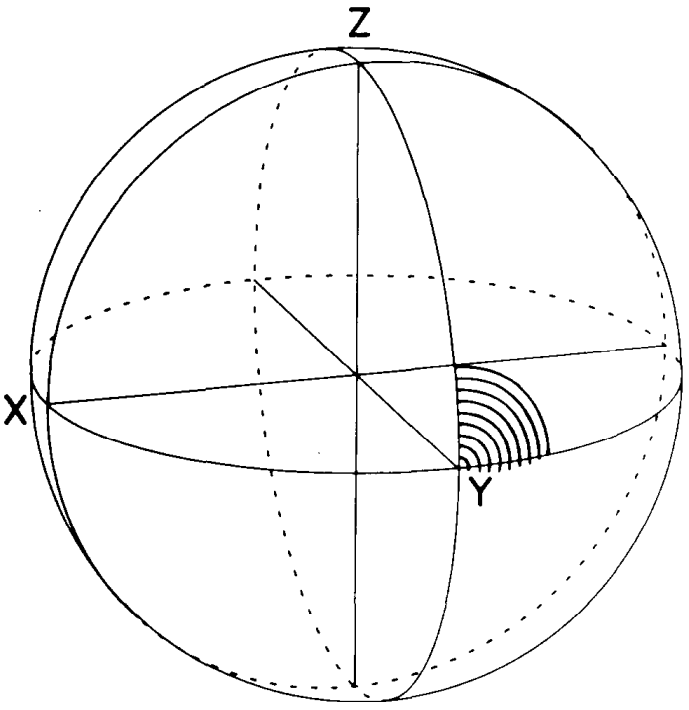

FIG. 3. Trajectories of a family of magnetization vectors during a 90°(X), 110°(Y) sequence representing pulse length missets between 0.8 and 1.0 times the nominal setting. Note the very small residual Z magnetization at the end of the sequence.

Compensation for Resonance Offset

It was demonstrated several years ago that a simple 90° pulse has a built-in compensation for resonance offset effects if judged only on the residual Z component of magnetization after the pulse (*3*). The reason is that the tilt of the effective field is largely compensated by the increase in H_{eff} as ΔH is increased. This can be illustrated by following a family of magnetization vectors representing a range of offsets ΔH and by plotting the loci of the tips of these vectors at various stages of their nutation about H_{eff} (Fig. 4). The curvature of the final locus is very small, so that it fits very close to the equator of the rotating reference frame. The phase errors are large and essentially a linear function of ΔH.

Should it be necessary to reduce these Z components even further, an improvement can be achieved with a composite two-pulse sequence. The two pulses act in opposite senses, and between them the nuclei are allowed to precess for a carefully chosen period τ, which introduces a curvature of the locus calculated to cancel the slight curvature of the final locus of Fig. 4. The time evolution is illustrated in Fig. 5. A 10°($-X$) pulse initiates the sequence and free precession for a period τ generates the locus $s-s'$. Then a 100°($+X$) pulse carries the family of vectors toward the XY plane, the final locus $t-t'$ lying very close to the equator. For a given offset ΔH, the amount of tilt of the effective field depends on the intensity of H_1, so the choice of τ for the best compensation depends on the value of H_1. For all of the pulse sequences described here, the radiofrequency field has been taken to be given by $\gamma H_1/2\pi =$ 10 kHz. With this condition good compensation is achieved with $\tau = 9$ μsec. The

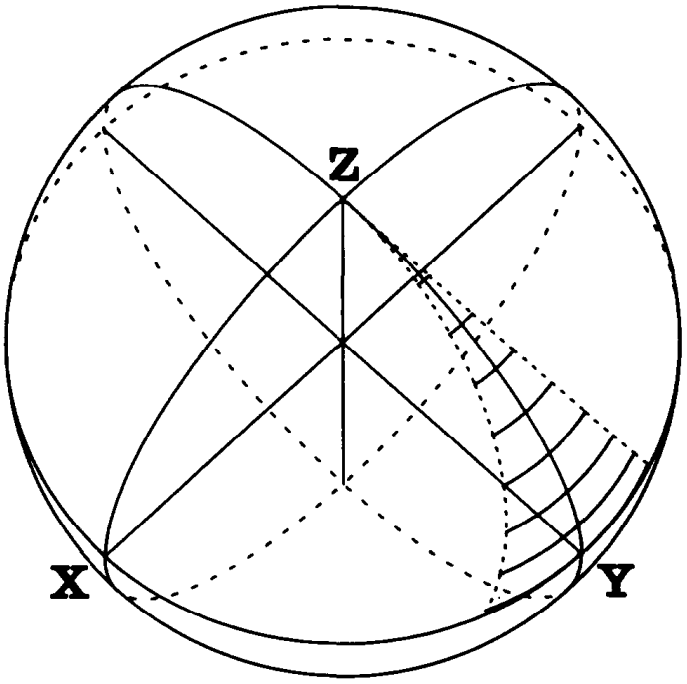

FIG. 4. The self-compensating effect of a conventional 90° pulse. A family of magnetization vectors representing resonance offsets $\Delta H/H_1$ from -0.33 to $+0.33$ has been considered, the locus of the tips of these vectors has been drawn at regular intervals during the pulse (full lines). Note that this locus coincides quite closely with the equatorial plane at the end of the pulse.

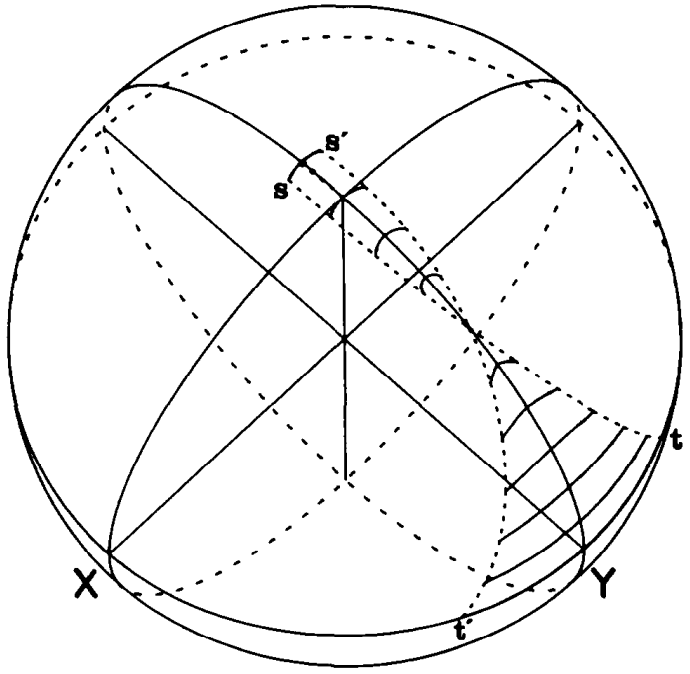

FIG. 5. Compensation of resonance offset effects with a composite $10°(-X)$, τ, $100°(+X)$ sequence. The period of free precession τ is chosen so as to minimize the residual Z magnetization after the pulse. With $\gamma H_1/2\pi = 10$ kHz, $\tau = 9$ μsec. As in Fig. 4, the full lines represent loci of the tips of a family of magnetization vectors corresponding to $\Delta H/H_1$ from -0.33 to $+0.33$.

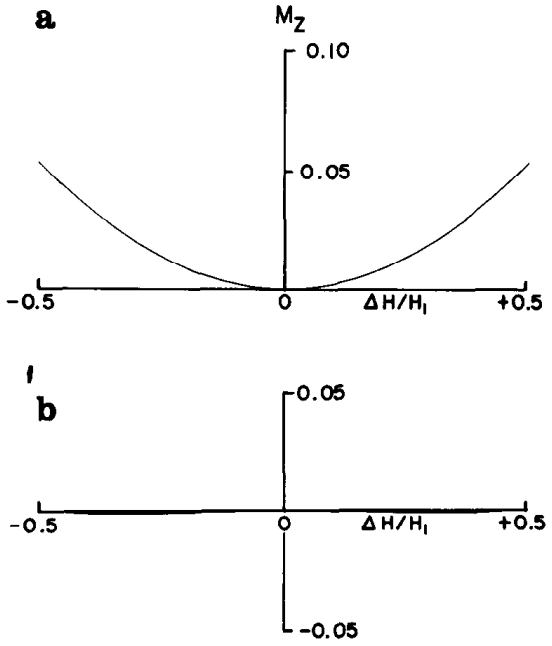

FIG. 6. Compensation for resonance offset effects with a $10°(-X)$, τ, $100°(+X)$ composite pulse. The residual Z magnetization after a conventional $90°(+X)$ pulse (a) is compared with that after the composite sequence (b).

improvement in the residual Z component after the pulse is shown in Fig. 6 as a function of the offset parameter $\Delta H/H_1$. For the conventional single 90° pulse (Fig. 6a) there is an approximately parabolic dependence whereas with the composite $10°(-X)$, τ, $100°(+X)$ sequence (Fig. 6b) the curve is very much flatter.

"*Spin Knotting*"

The two-pulse sequence of the previous section provides the clue for a composite sequence which compensates for both Z-component errors and phase errors at the same time. This has important applications in spin-locking experiments (4–6) where either phase errors or residual Z components after the first 90° pulse preclude the proper alignment of the magnetization vectors along the spin-locking field. The result is that not all magnetization components relax with the expected time constant $T_{1\rho}$ but precess about the spin-locking field undergoing the nutational motion first described by Torrey (*7*).

The time evolution of the magnetization vectors during this three-pulse sequence is most clearly visualized if the variable parameters (pulse lengths and interpulse intervals) are not at first optimized. The algebraic sum of the three nominal flip angles is maintained at +90°, so that an isochromat at exact resonance is carried from the Z axis to the Y axis. There are thus four independent variable parameters.

The three pulses carry the spins clockwise, counterclockwise, and clockwise about the X axis. The first pulse is $20°(+X)$ and is short enough that tilt effects are almost negligible. It is followed by free precession for a period of 30 μsec (Fig. 7). A family

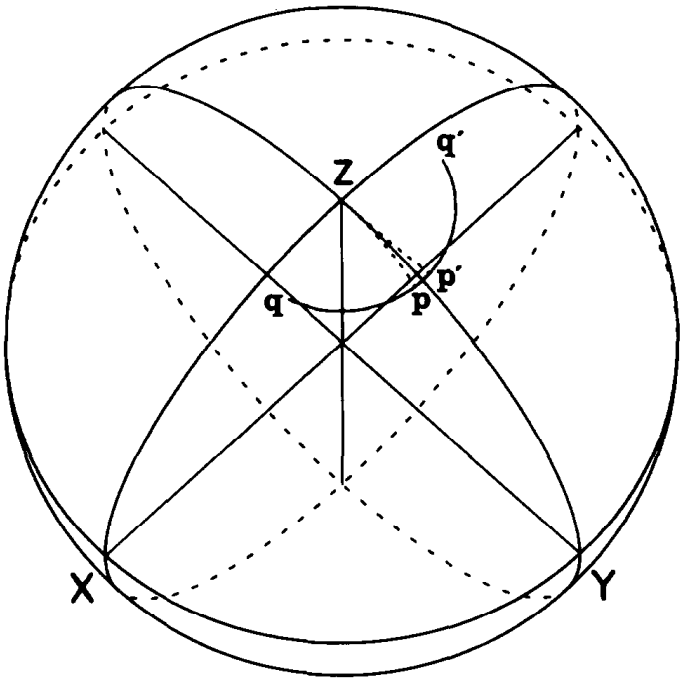

FIG. 7. "Spin-knotting" pulse sequence. A 20°(+X) pulse carries a family of magnetization vectors forward until the tips of the vectors lie along the locus $p-p'$. A period of 30 μsec free precession allows this locus to expand along $q-q'$. A range of offsets $\Delta H/H_1 = -0.5$ to $+0.5$ has been considered.

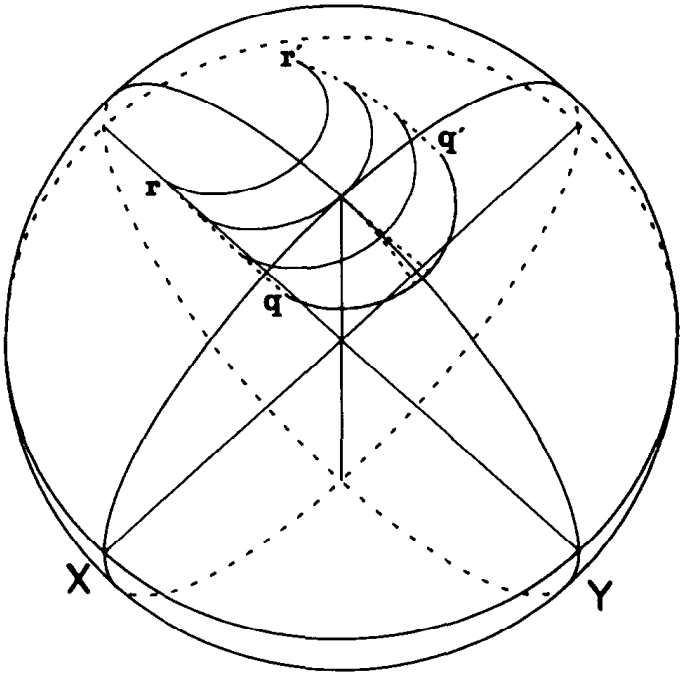

FIG. 8. "Spin-knotting" pulse sequence. The second pulse, 30°(−X), carries the locus $q-q'$ back to $r-r'$.

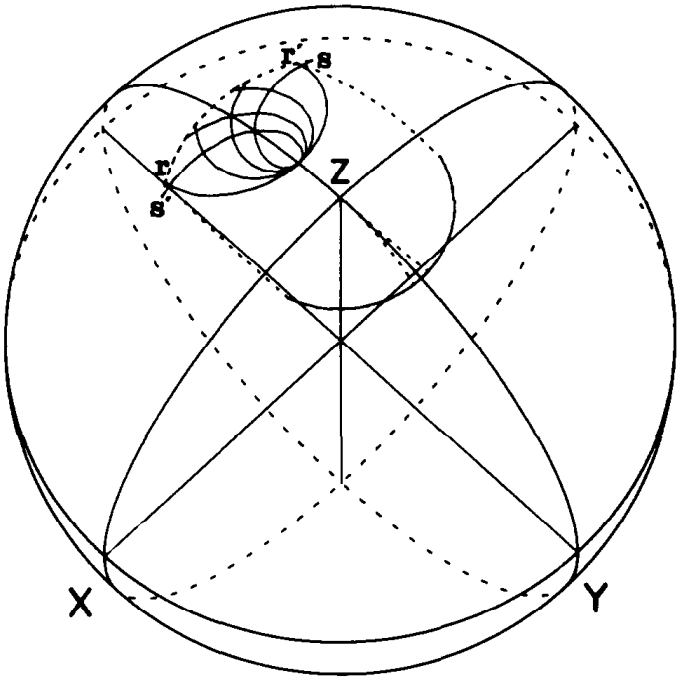

FIG. 9. "Spin-knotting" pulse sequence. The second period of free precession, 30 μsec in duration, allows the locus $r-r'$ to fold in upon itself, forming a loop $s-s'$ where the relative positions of "high-field" and "low-field" vectors have been reversed.

of isochromats is considered covering the range $\Delta H/H_1$ from -0.5 to $+0.5$, and gives rise to a locus $q-q'$. The second pulse, $30°(-X)$, carries this arc back over the pole $(+Z)$ leaving a locus $r-r'$ (Fig. 8). There is then a further 30-μsec period of free precession, during which this arc folds in upon itself, reversing the relative positions of clockwise and counterclockwise precessing vectors and giving the locus $s-s'$ (Fig. 9). Finally the third pulse, $100°(+X)$, carries this looped locus forward over the pole, converting it into a bow in the process $(t-t')$ (Fig. 10). A clearer view of the final locus $t-t'$ can be seen in Fig. 11 from a different angle.

This "knot" may be tightened by suitable adjustment of the parameters. Shortening the first pulse while lengthening the second improves the compensation. It may be noted that then the relative amplitudes of the three pulses follow roughly the form of one-half of a sinc curve, the form of excitation which would be expected to give uniform excitation in the limit of a linear response by the spins. Trial-and-error simulations indicate that a near-optimum sequence is

$$10°(+X), \quad 40\ \mu\text{sec}, \quad 60°(-X), \quad 11\ \mu\text{sec}, \quad 140°(+X).$$

Figure 12 shows the final locus to be a tight loop at the end of this sequence. With this sequence the residual Z component of magnetization after the composite pulse is quite small for a range of offset parameters from -0.3 to $+0.3$ as seen in Fig. 13 and the phase errors are similarly compensated (Fig. 14).

The compensation of phase errors (dispersion-mode components) has been tested experimentally in Fig. 15, which shows the offset dependence of a single carbon-13

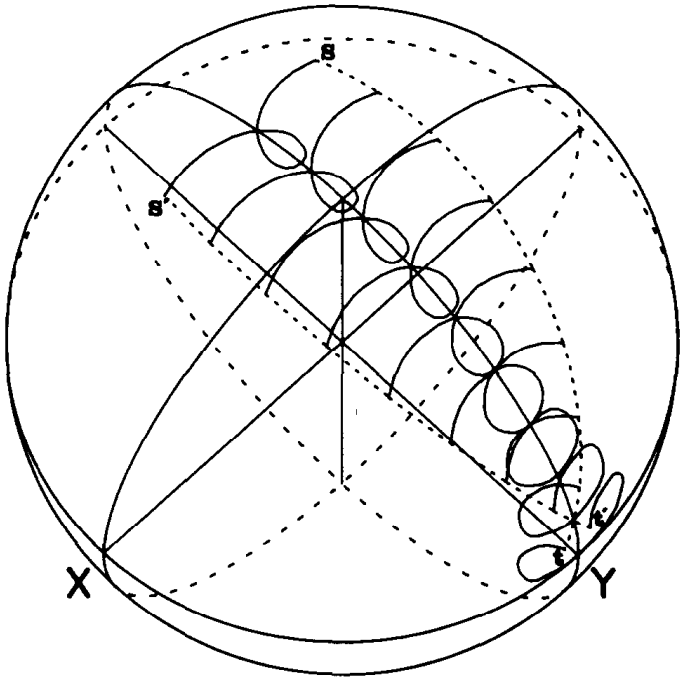

FIG. 10. "Spin-knotting" pulse sequence. The third pulse $100°(+X)$ carries the looped locus $s-s'$ forward toward the $+Y$ axis, leaving it in the form of a bow $t-t'$.

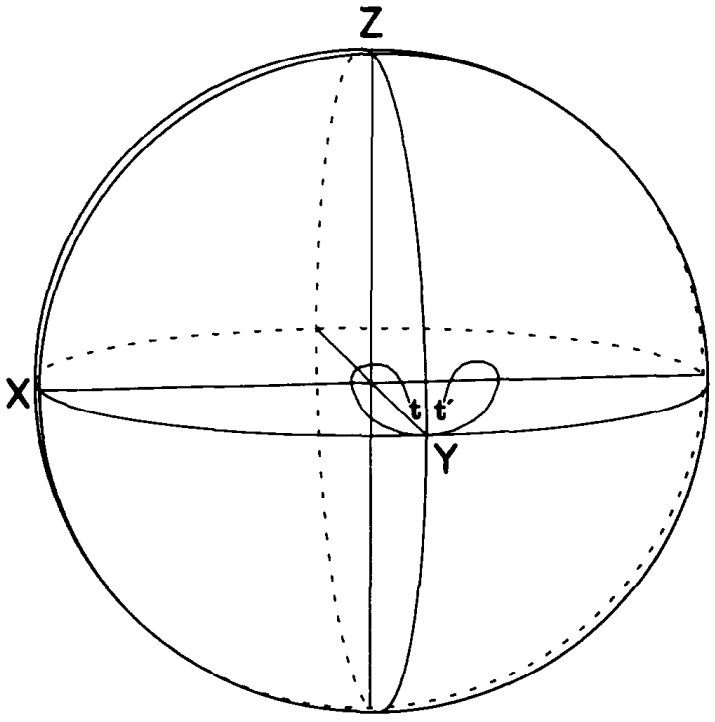

FIG. 11. The final locus of the tips of the magnetization vectors after a "spin-knotting" sequence, viewed from the $+Y$ axis.

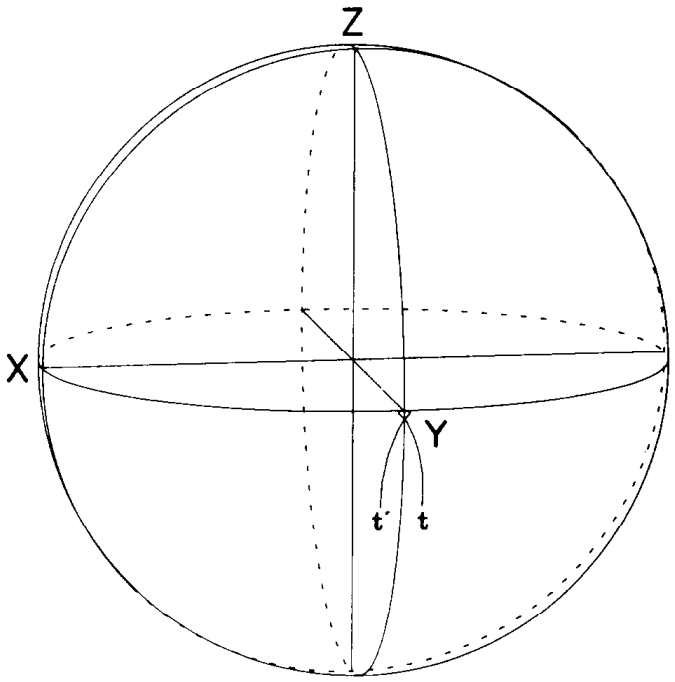

FIG. 12. The final locus after an optimized "spin-knotting" sequence, 10°(+X), 40 μsec, 60°(−X), 11 μsec, 140°(+X). Note that the "bow" of Fig. 11 has been tightened so that vectors representing small offsets are grouped close to the +Y axis.

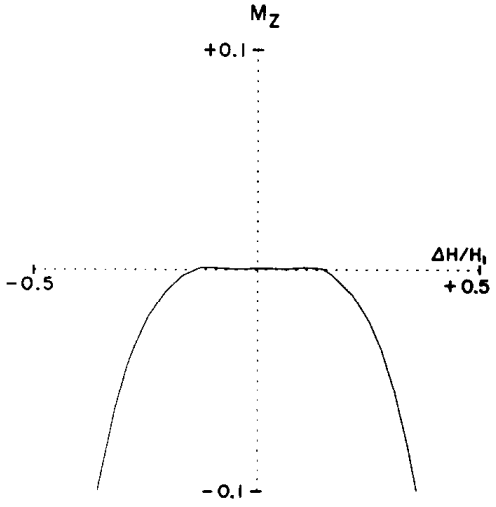

FIG. 13. The compensation of resonance offset effects achieved with the optimized "spin-knotting" sequence, bringing the Z magnetization after the composite pulse close to zero for small offsets.

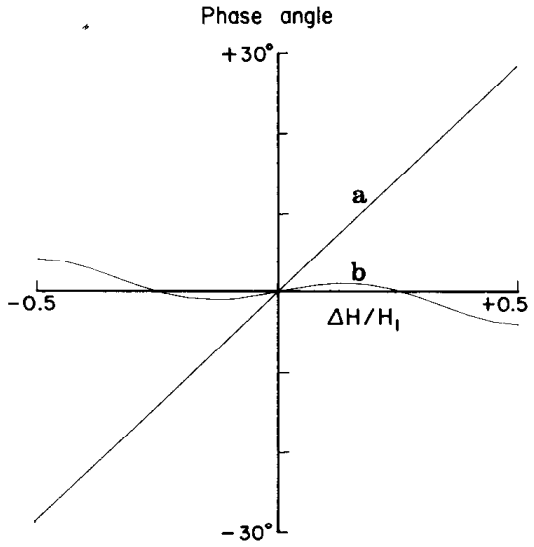

FIG. 14. The compensation of resonance offset effects achieved with the optimized "spin-knotting" sequence. The phase errors after a conventional 90°(+X) pulse (a) are compared with those at the end of the composite sequence (b).

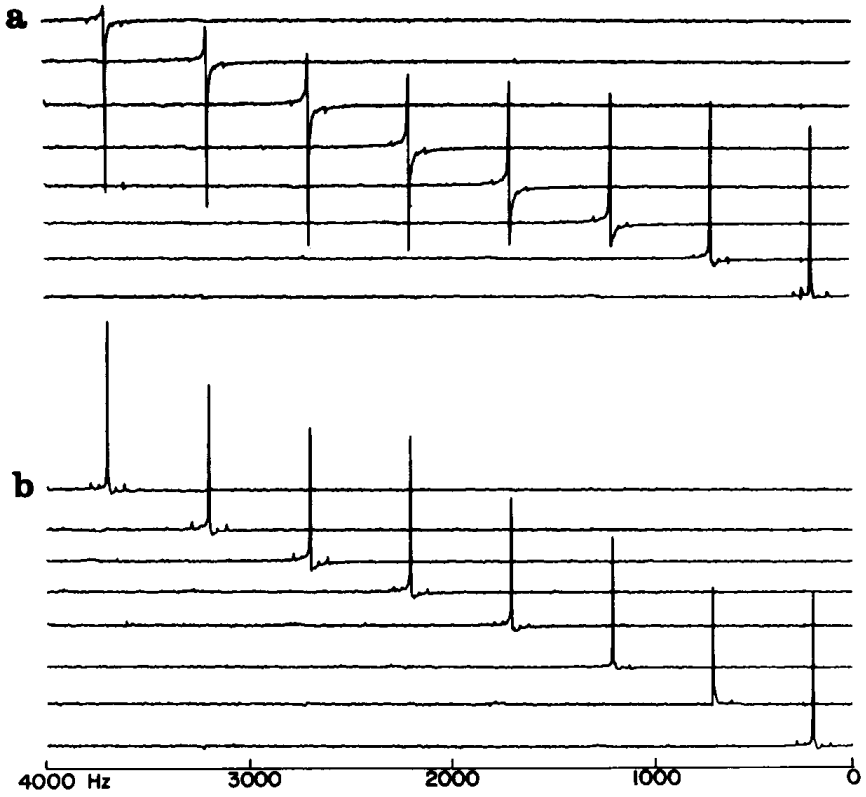

FIG. 15. An experimental test of the compensation of phase errors by the optimized "spin-knotting" sequence. (a) After a conventional 90°(+X) pulse, a signal which is correctly phased close to resonance rapidly acquires phase errors as it is moved away from resonance. (b) After the composite sequence, these phase errors are effectively compensated.

signal after a conventional 90° pulse (Fig. 15a) compared with the same series of signals after the near optimum spin-knotting sequence (Fig. 15b). Note the much better phasing in the latter series.

Spin-Locking Experiments

Of the possible applications of the composite sequence described in the previous section, the spin-locking experiment is probably the most important since it relies on all isochromats being aligned along the appropriate effective field H'_{eff}, irrespective of the offset ΔH. Failure to meet this condition changes the rate of decay and introduces oscillatory components onto the signal when it is followed as a function of the spin-locking time. The experiment can be considered to be divided into two parts, the preparation (alignment of isochromats along $+Y$) and the spin-locking period. For the experiment proposed here, H_1 is approximately twice as strong during the preparation period as during spin locking; hence the effective field during preparation (H_{eff}) is different from that during spin locking (H'_{eff}).

Suppose for the sake of this section that essentially perfect alignment has been achieved along the Y axis (for isochromats in a certain offset range) by a "spin-knotting" composite pulse. There remains the problem of turning each isochromat so as to align it along its characteristic H'_{eff}, since the direction of H'_{eff} varies with offset ΔH. Fortunately there is a simple trick to accomplish this. A 180°(Y) pulse (Fig. 16) carries each isochromat in a different arc, depending on θ and on H_{eff}, slightly overshooting the YZ plane. A very short period of free precession corrects this overshoot, leaving the isochromats fanned out along an arc in the YZ plane. Now if the radiofrequency field intensity H_1 is suitably reduced during the spin-locking period, each new H'_{eff} can be made to correspond quite closely to the direction of the appropriate isochromat. The choice of reduction factor is a mild compromise, depending on the offset range to be covered, but 0.48 is found to be suitable for offset parameters up to ±0.5. For offsets small enough that $\tan\theta \simeq \theta$, the reduction factor is just 0.5. To date, this appears to be the most promising method of preparing nuclear spin magnetization vectors at different resonance offsets so that they may be effectively "locked" by a continuous radiofrequency field in order to measure the transverse relaxation times.

An appreciation of the improvement to be achieved can be obtained by following the trajectories of typical magnetization vectors by computer simulation. Four vectors, representing offsets $\Delta H/H_1 = \pm 0.33$ and ± 0.17 were allowed to evolve according to a spin-knotting sequence and then a 180°(Y) pulse. After free precession for 3 μsec, a simulated radiofrequency field was applied along the $+Y$ direction reduced in intensity by a factor 0.48. Figure 17 maps out the spiral paths of the four vectors as they precess about their appropriate effective fields. These are to be compared with the precession of much higher amplitude for a vector with offset parameter 0.33 prepared with a conventional 90°(X) pulse and the usual spin-locking field applied along the $+Y$ axis (Fig. 18). This trajectory along the surface of a wide-angle cone resembles the nutational motion described by Torrey (*7*) as much as the "forced precession" described by Solomon (*5, 6*) and hence involves a complicated combination of spin–spin and spin–lattice relaxation.

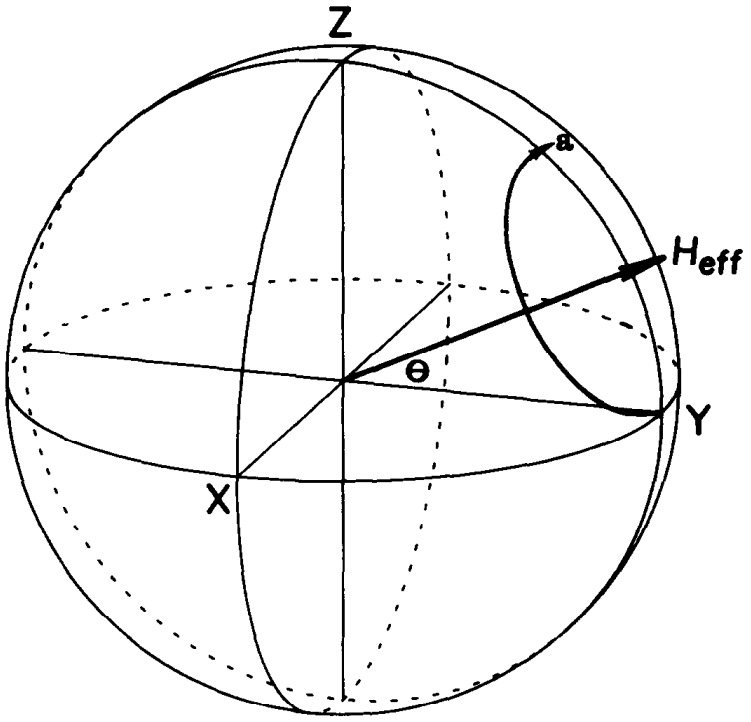

FIG. 16. Preparation for spin locking along the effective field H'_{eff}. All vectors are assumed to have been aligned along $+Y$ by a "spin-knotting" sequence. A $180°(+Y)$ pulse then carries each vector along a different arc according to the appropriate offset ΔH, slightly overshooting the ZY plane (a). A very short period of free precession cancels this overshoot. The radiofrequency field intensity is then reduced to about half its normal value, so that the new effective field H'_{eff} is aligned along the appropriate magnetization vector, the angle θ being approximately doubled.

COMPOSITE 180° PULSES

Pulses of 180° are used for two main purposes, to turn magnetization vectors lying in the XY plane into mirror image positions with respect to the H_1 axis, or to take magnetization vectors from the $+Z$ to the $-Z$ axis in order to create a population inversion and an interchange of spin states. It has not yet been possible to devise a composite sequence suitable for this first application, the 180° refocusing pulse. Fortunately the well-known Meiboom–Gill modification (*8*) or the related phase-alternation scheme (*9*) satisfactorily compensates the effects of radiofrequency field inhomogeneity and resonance offset at the time of the even-numbered echoes.

Composite 180° pulses designed for population inversion are considered here. A brief account of a $90°(X), 180°(Y), 90°(X)$ sequence was presented in an earlier note (*10*). This composite pulse compensates for spatial inhomogeneity and resonance offset effects. Indeed it is readily seen that the compensation for pulse length error would be exact if the $180°(Y)$ pulse were perfect; that is, a $\theta°(X), 180°(Y), \theta°(X)$ sequence is equivalent to a single 180° pulse for all values of θ. If θ approaches 90°, the excursions during the $180°(Y)$ pulse are small, and the effects of imperfections in the $180°(Y)$ pulse are minimized. Hence for $90°(X), 180°(Y), 90°(X)$ sequences,

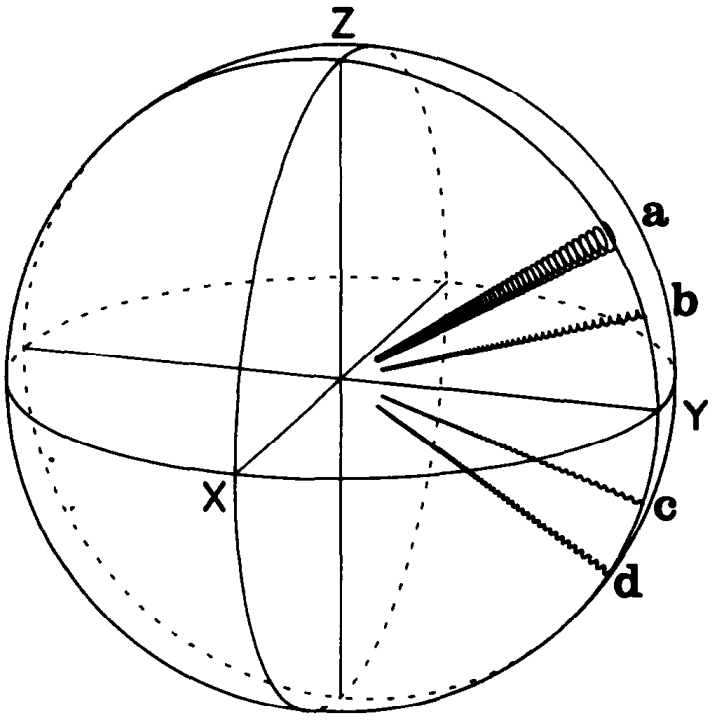

FIG. 17. The spiral trajectories of typical magnetization vectors during spin-locking experiments where the preparation involved the "spin-knotting" sequence, a 180°(+Y) pulse, a short period of precession, and a reduced spin-locking field 0.48 H_1, according to the prescription of Fig. 16. The four trajectories have been calculated for offset parameters $\Delta H/H_1$ equal to (a) +0.33, (b) +0.17, (c) −0.17, (d) −0.33.

small discrepancies in flip angle are particularly well compensated. Naturally this high degree of compensation is not maintained for sample regions where H_1 is very weak, but such regions contribute very little signal.

The degree of compensation can be illustrated by plotting contours of Z magnetization after the pulse as a function of pulse length error (H_1/H_1°) and offset parameter ($\Delta H/H_1$). It will be noted that all these contour diagrams are symmetrical with respect to offsets above and below the transmitter frequency. In the case of a three-pulse sequence the reasons for this property are not immediately obvious, but lie deep within the symmetry properties of the elements of the three rotation matrices. In the Appendix it is shown that the resultant Z magnetization possesses such symmetry after any three-pulse sequence of the form $\alpha(X)$, $\beta(Y)$, $\alpha(X)$ only if the first and last pulses are identical in length and flip axis. No such symmetry exists either in the final values of the X and Y components of magnetization or in the intermediate trajectories of the magnetization vectors.

Figure 19 shows that a conventional 180°(X) pulse has very little tolerance of pulse length error or resonance offset; note the small area within which the Z magnetization after the pulse is greater than 99% of M_0. This should be compared with the corresponding contour diagrams for the composite 90°(X), 180°(Y), 90°(X) sequence illustrated in Fig. 20, where pulse length errors four times larger can be accommodated within the same 99% contour. Note that it is only near the top of this

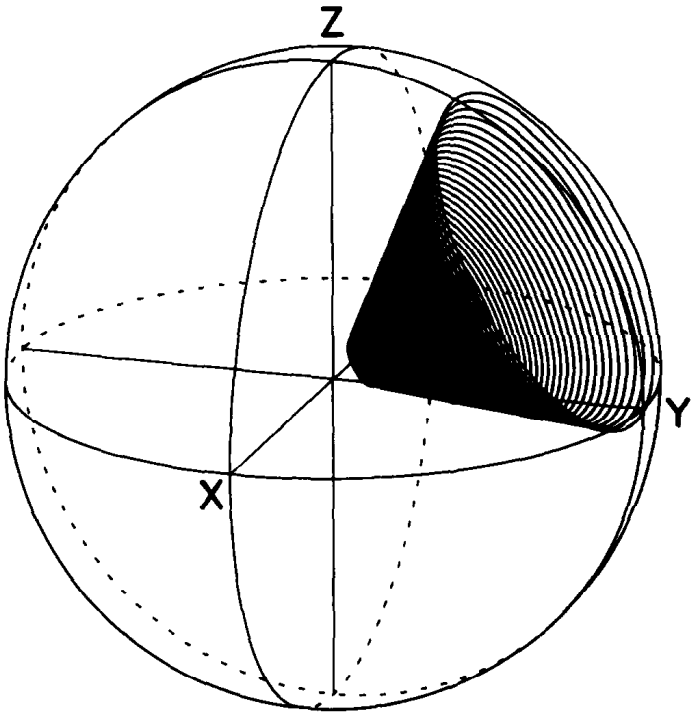

FIG. 18. The corresponding spiral trajectory of a typical magnetization vector ($\Delta H/H_1 = +0.33z$ during a spin-locking experiment where the preparation involved a conventional 90°(+X) pulse. These large excursions cause large errors in the derived relaxation time.

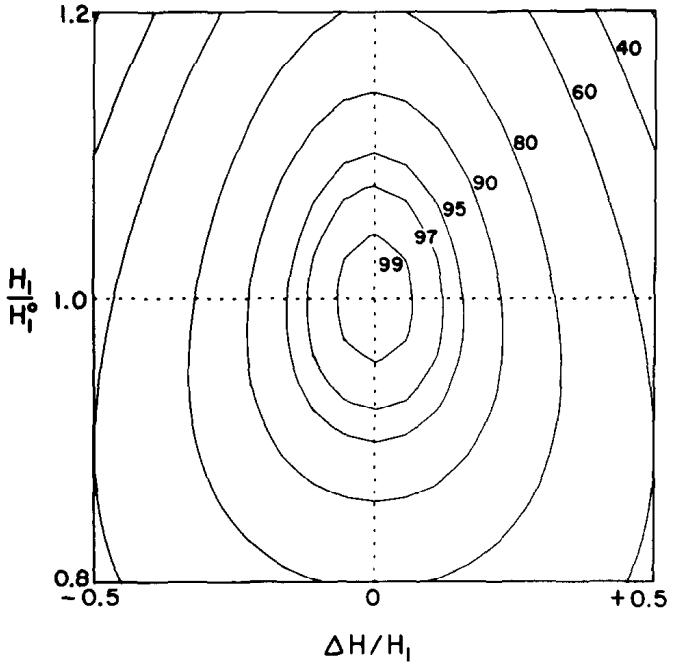

FIG. 19. The contours of residual Z magnetization (expressed as a percentage of M_0) after a conventional 180°(+X) pulse, as a function of pulse length misset H_1/H_1^0 and resonance offset $\Delta H/H_1$.

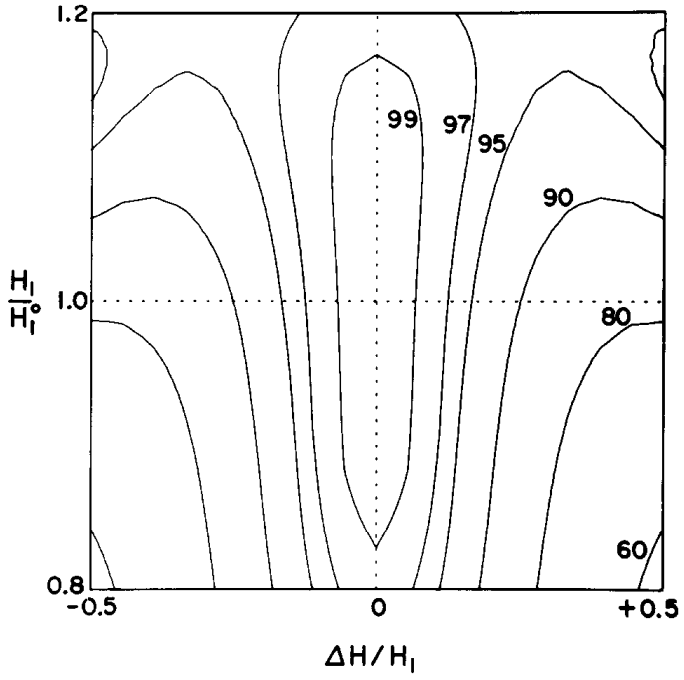

FIG. 20. Contours of residual Z magnetization after a composite 90°(+X), 180°(+Y), 90°(+X) sequence. Note that in comparison with the contours of Fig. 19, this diagram shows a higher tolerance of pulse length errors, and therefore of spatial inhomogeneity of the radiofrequency field.

diagram that there is much compensation for resonance offset effects. This is the clue that better compensation for offset can be achieved by deliberately increasing the pulse lengths beyond their nominal settings of 90 and 180°. It is not necessary to increase the two pulses in proportion, and in fact good results are obtained by increasing only the second pulse to give the composite sequence

$$90°(X), 240°(Y), 90°(X).$$

The trajectories of vectors representing a range of offset from $\Delta H/H_1 = 0.4$ to $\Delta H/H_1 = 0.6$ are followed in Fig. 21; the increased length of the second pulse is seen to compensate for the fact that it operates about a tilted axis. This family of vectors terminates quite close to the $-Z$ axis, although a conventional 180°(X) pulse would have taken these vectors far from the YZ plane. Figure 22 shows the contours of Z magnetization after the 90°(X), 240°(Y), 90°(X) sequence. There is a wide range of offset parameters which give only a small error in M_Z. In fact there is a roughly T-shaped area where the Zmagnetization remains above 97% of its ideal value. Compensation for spatial inhomogeneity of H_1 is therefore good, for it is the *low* values of H_1 which require compensation, representing sample regions remote from the center of the transmitter coils. Figure 23 illustrates how the increased length of the second pulse compensates for a range of weaker-than-normal H_1 fields arising from spatial inhomogeneity, turning all the magnetization vectors down toward the $-Z$ axis.

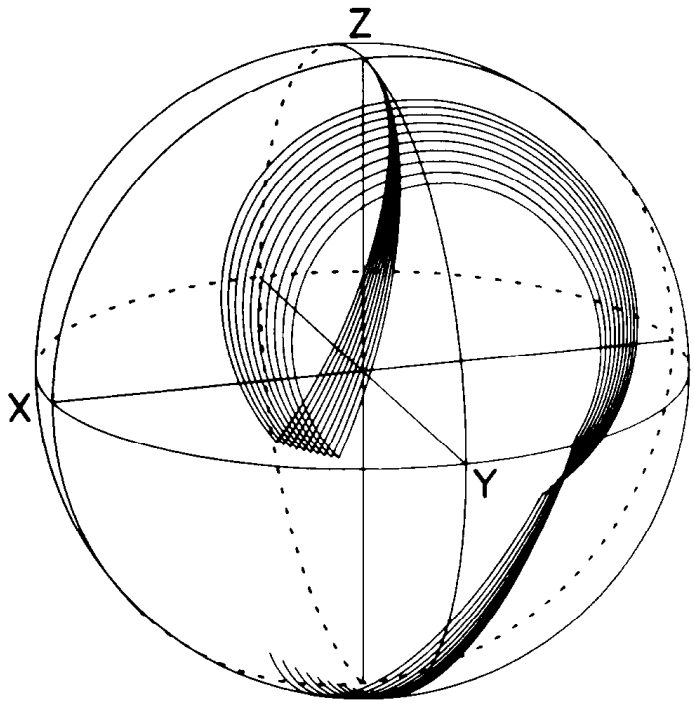

FIG. 21. Trajectories of a family of magnetization vectors (representing offset parameters $\Delta H/H_1$ between 0.4 and 0.6) during a composite pulse sequence 90°(+X), 240°(+Y), 90°(+X). Note that these trajectories terminate much closer to the $-Z$ axis than those after a single 180°(+X) pulse.

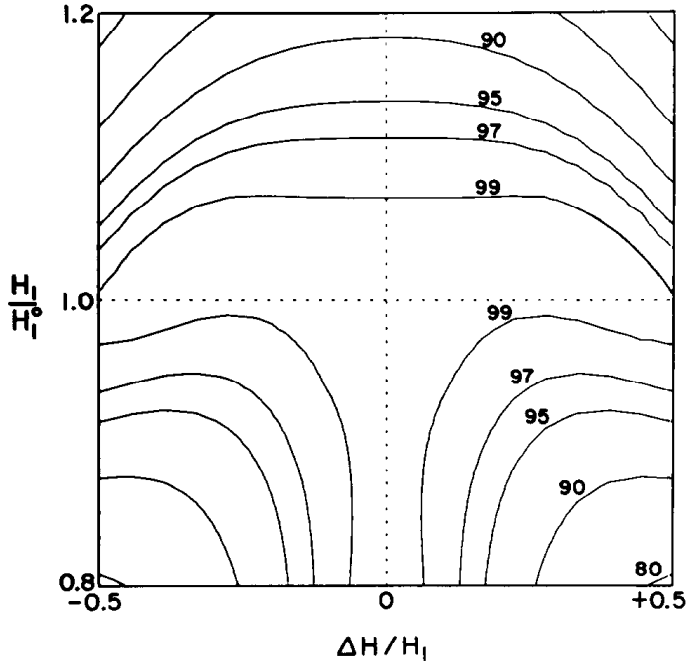

FIG. 22. Contours of residual Z magnetization after a composite 90°(+X), 240°(+Y), 90°(+X) sequence. Note the high tolerance of resonance offset $\Delta H/H_1$ as well as pulse length misset below the nominal value. In a large T-shaped region M_Z is held within 1% of M_0.

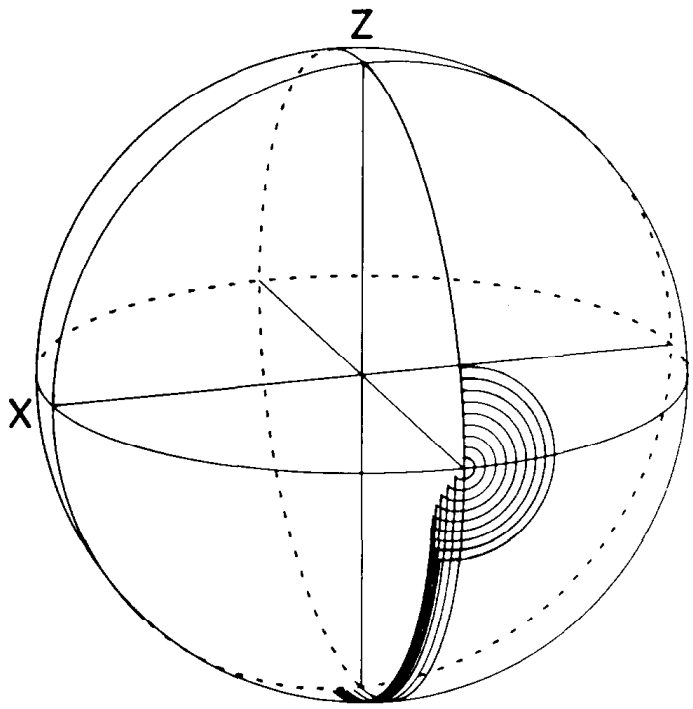

FIG. 23. Compensation of pulse length errors in the composite $90°(+X)$, $240°(+Y)$, $90°(+X)$ sequence. A family of magnetization trajectories has been traced out for pulse lengths between 0.8 and 1.0 times the nominal value. Note how the termini are grouped close to the $-Z$ axis.

An experimental test of the population inversion obtained with the composite pulse sequence can be made very simply by monitoring the Z magnetization with a subsequent 90° pulse, alternating the phase to cancel transverse magnetization (*11*), and allowing no time for spin–lattice relaxation. Figure 24 shows the equilibrium Z magnetization monitored by a single 90° pulse (a), the imperfect inversion achieved after a conventional 180° pulse (b), and the essentially complete inversion achieved after a composite $90°(X)$, $200°(Y)$, $90°(X)$ sequence (c). Spatial inhomogeneity effects were minimized by the use of a small spherical bulb sample, in order to test the effect of resonance offset, $\Delta H/H_1 = 0.4$.

A preliminary report (*10*) on composite 180° pulses utilized the null method for determining spin–lattice relaxation times as a test of the efficiency of population inversion. Pulse imperfections lead to imperfect inversion and a systematic underestimate of the spin–lattice relaxation time if calculated from the time at which the signal passes through the null. Thus if the true spin–lattice relaxation time is known, the timing of the null is a sensitive test of pulse imperfections. The original experiments (*10*) used a $90°(X)$, $180°(Y)$, $90°(X)$ sequence, which, as has been shown above, is not optimized for compensation of the effects of resonance offset. The $90°(X)$, $240°(Y)$, $90°(X)$ composite sequence gives better results.

An experimental test of the effectiveness of this composite sequence was made on a small spherical sample of methyl iodide by following the spin–lattice relaxation of the singlet carbon-13 signal, decoupled from protons. First a careful determination

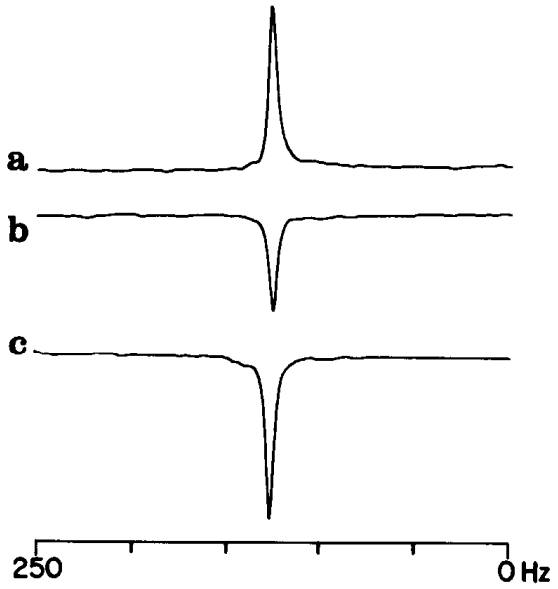

FIG. 24. Experimental test of the composite $90°(+X), 200°(+Y), 90°(+X)$ pulse sequence. The signals were all observed by means of a conventional $90°(+X)$ "read" pulse. The initial conditions were (a) Boltzmann equilibrium, (b) population inversion by a conventional $180°(+X)$ pulse, (c) population inversion by the composite sequence. A small bulb sample was used, and the offset parameter was $\Delta H/H_1 = 0.4$.

of the spin–lattice relaxation time by inversion–recovery was made, using a semi-logarithmic plot of the difference signal $S_\infty - S_t$. This method is known to be insensitive to pulse imperfections provided that the phase of the monitoring 90° pulse is alternated (*11*). A result of $T_1 = 13.4 \pm 0.1$ sec was obtained.

With this knowledge of the "true" T_1 it was possible to use the null point (determined from two measurements which bracketed the null) as a measure of pulse imperfections. Table 1 illustrates the dependence of the systematic error on the resonance offset for the case of a conventional single $180°(X)$ pulse, compared with a

TABLE 1

APPARENT SPIN-LATTICE RELAXATION TIMES DETERMINED BY THE NULL METHOD: EFFECT OF RESONANCE OFFSET

$\gamma\Delta H/2\pi$ (kHz)	$\Delta H/H_1$	Conventional pulse T_1 (sec)	Composite pulse T_1 (sec)
0	0.00	13.3 (−1)[a]	13.4 (<1)
1	0.09	13.0 (−4)	13.4 (<1)
2	0.18	12.0 (−11)	13.4 (<1)
3	0.27	10.8 (−20)	13.4 (<1)
4	0.36	9.7 (−28)	13.1 (−2)

[a] Systematic error (%) with respect to the value $T_1 = 13.4$ sec measured by careful inversion–recovery experiments and least-squares fitting to an exponential.

TABLE 2

APPARENT SPIN–LATTICE RELAXATION TIMES DETERMINED BY THE NULL METHOD: EFFECT OF PULSEWIDTH MISSET

t_p/t_p°	α (°)	Conventional pulse T_1 (sec)	Composite pulse T_1 (sec)
1.0	180	13.3 (−1)[a]	13.4 (<1)
0.9	162	12.8 (−5)	13.4 (<1)
0.8	144	12.1 (−10)	13.3 (−1)
0.7	126	11.0 (−19)	13.3 (−1)
0.6	108	6.2 (−54)	12.1 (−10)
0.5	90	–[b]	10.2 (−24)

[a] Systematic error (%) with respect to the value $T_1 = 13.4$ sec measured by careful inversion–recovery experiments and least-squares fitting to an exponential.

[b] Signal not inverted; null not observed.

composite 90°(X), 240°(Y), 90°(X) sequence. The apparent T_1 values showed large errors when the conventional pulse was used, increasing with the offset parameter $\Delta H/H_1$, while the composite sequence greatly reduced these errors, holding them below 1% for most of the offset range.

The effect of spatial inhomogeneity was then simulated by deliberately missetting the flip angles α used for population inversion. Initially the conventional pulse was 180°(X) and the composite pulse 90°(X), 240°(Y), 90°(X). Then all four pulse widths were reduced in the same proportion in order to follow the effects of incomplete inversion, the monitoring pulse being kept fixed throughout at 90°(X). This introduced large systematic errors into the apparent spin–lattice relaxation times determined from the null point if the conventional single pulse was used, but much smaller errors when the composite sequence was employed (Table 2). Even when the three pulses were set at 70% of their nominal widths, the composite sequence held the error within 1%. It may be inferred from these results that the corresponding errors due to spatial inhomogeneity effects should be similarly reduced (Table 3).

Good compensation may therefore be achieved for resonance offset effects or for radiofrequency inhomogeneity, but when both types of imperfection occur simultaneously, the contour diagram (Fig. 22) indicates that compensation is less effective. For high-resolution spectra with lines spread over a wide frequency range, it appears likely that the offset effect will be the more serious.

EXPERIMENTAL

The practical tests of various composite pulse sequences were carried out on a Varian CFT-20 spectrometer using carbon-13 signals from enriched methyl iodide. Only minor modifications are necessary to implement this technique, principally the provision of a second transmitter channel shifted in phase by 90° (*12*). The remaining changes are accomplished by machine code program modifications, one of the chief

TABLE 3

COMPOSITE PULSE SEQUENCES

Composite sequence	Equivalent	Compensation	Application
$90°(X), 90°(Y)$ or $90°(X), 110°(Y)$	$90°(X)$	H_1 inhomogeneity	Saturation[a]
$10°(-X), \tau, 100°(+X)$[b]	$90°(X)$	ΔH	Saturation[a]
$10°(+X), \tau_1, 60(-X), \tau_2, 140°(+X)$	$90°(X)$	ΔH	Saturation[a]
$10°(+X), \tau_1, 60°(-X), \tau_2, 140°(+X), 180°(+Y), \tau_3$	$90°(X)$	ΔH	Preparation for spin-locking
$90°(X), 180°(Y), 90°(X)$ or $90°(X), 240°(Y), 90°(X)$	$180°(X)$	ΔH or H_1 inhomogeneity	Population inversion
$90°(+X), \theta°(+Y), 90°(-X)$	$\theta°(+Z)$	None	Rotation about Z

[a] For a saturation–recovery or a progressive saturation experiment to measure T_1.

[b] τ represents a period of free precession.

difficulties on this instrument being to ensure that the interpulse intervals were sufficiently short when free precession between pulses had to be avoided. In practice the minimum interpulse interval attainable was 11 μsec. More sophisticated pulse programmers would be useful in this regard.

A sensitive and rapid experimental check of the accuracy of the 90° phase shift is provided by the composite $90°(X), 180°(Y), 90°(X)$ sequence applied to a resonance close to the transmitter frequency ($\Delta H \ll H_1$) on a small spherical sample where a spatial inhomogeneity of H_1 can be neglected. The three pulse lengths must be properly calibrated for this test. If the phase shift is correct and the second pulse is applied about the Y axis, then the detected signal should be a null, the magnetization vector being aligned along $-Z$. If there is a small deviation δ from the 90° phase shift, the second pulse carries the magnetization vector away from the YZ plane to a position where it subtends an angle 2δ with respect to the $+Y$ axis. After the third pulse this is translated into a residual (negative) dispersion-mode signal of amplitude $M_0 \sin 2\delta \simeq 2M_0\delta$ for small angles δ. Thus the amplitude and sign of this residual signal can be used as a test for the amount of the sense of the dephasing of the $180°(Y)$ pulse.

Pulsewidth calibration was carried out by searching for the condition which gave a null signal after a complete rotation, according to Eq. [3]. The pulsewidths for 90 and 180° pulses were reduced in proportion, since the "droop" in the intensity of H_1 over these time periods had been adjusted to be negligible. Pulse droop is a feature designed to protect the output transistors in the transmitter circuit; an alternative scheme consisting of a period of constant amplitude H_1 followed by a delayed droop was incorporated as a modification in the spectrometer used.

DISCUSSION

The concept of a composite pulse is not really new; a "2–1–4" sequence was used by Redfield (*13*) to achieve frequency selectivity, and quite complicated pulse sequences are commonplace in solid-state NMR (*14*). However, their use in

high-resolution NMR has been extremely limited. The present work emphasizes the use of composite pulses to compensate the two common pulse imperfections, H_1 inhomogeneity and resonance offset effects. However, this is unlikely to be the only application, because the principle appears to be quite general. Whereas a conventional single pulse is described by two parameters, the flip angle α and the axis along which H_1 is directed, a composite pulse involves many more independently variable parameters (including periods of free precession between pulses) and its applications are correspondingly more flexible. The adjustment of these variable parameters can be carried out either by trial-and-error (aided by computer simulation), as in the "spin-knotting" sequence described above, or through a computer program to optimize these parameters according to some desired experimental criterion. It is nevertheless a good rule to keep the number of elements in the sequence to the minimum required to solve the problem.

One example will serve to illustrate that quite different applications are conceivable. Suppose that it becomes necessary to contrive a rotation of magnetization vectors by θ degrees about the Z axis of the rotating frame. For a high-resolution spectrum with several resonance lines, a simple free precession would not achieve this. Provided that the pulses can be considered ideal, then a $90°(+X)$, $\theta°(+Y)$, $90°(-X)$ composite sequence can be shown to be equivalent to $\theta°(+Z)$. This is readily appreciated by considering the behavior of the three magnetization components separately; M_Z remains unchanged while M_X and M_Y are rotated through $\theta°$ clockwise about the $+Z$ axis. There are several possible extensions of this principle.

Compensated 90° pulses should prove useful in spin–lattice relaxation experiments carried out by the saturation–recovery or progressive saturation techniques. Unfortunately, H_1 inhomogeneity and resonance offset effects cannot yet be compensated simultaneously, so a decision must be made about the relative importance of the two types of pulse imperfection. If spatial inhomogeneity of H_1 is the dominant factor in a particular experimental situation, then the $90°(X)$, $90°(Y)$ sequence (or an optimized variation) is indicated; if resonance offset effects are more critical, then the "spin-knotting" sequence is preferable.

Spin-echo methods of determining spin–spin relaxation times are often complicated by the modulation generated by homonuclear coupling (*15*), so the spin-locking experiment can be a simpler method of obtaining this relaxation information. However, there are practical limitations to the application of very strong spin-locking radiofrequency fields for periods of the order of seconds. Consequently, for high-resolution spectra with many lines, the tilt of the effective field H'_{eff} must be taken into account. It is suggested that the "spin-knotting" sequence might be used to prepare the nuclear magnetization vectors, leaving them suitably aligned along $+Y$, and then a 180° pulse would fan them out into an arc in the YZ plane, at which point a reduced H_1 field would be applied such that each individual isochromat is locked along its appropriate effective field H'_{eff}. Where radiofrequency heating is a severe problem, *three* levels of radiofrequency intensity could be employed—the full intensity for the short pulses in the preparation sequence, a significantly reduced H_1 for the $180°(Y)$ pulse, followed by a further twofold reduction for the spin-locking period.

The composite 180° pulse sequence can compensate for either H_1 inhomogeneity or resonance offset effects, although the correction is less effective where there is both an abnormally low flip angle and a large resonance offset. Once essentially complete population inversion can be guaranteed, the null method of determining spin–lattice relaxation times has much to recommend it. The method is fast because it requires no determination of the asymptotic signal S_∞, and the null point can be rapidly located by bracketing, using a linear interpolation (a very good approximation in this short section of the exponential recovery curve). It is a particularly effective method when there is already a good estimate of T_1 available, or when small changes in T_1 are being studied.

When composite 180° pulses are used for the "fast inversion–recovery" method (*16*), improved accuracy in the derived relaxation times is to be expected. In this mode, the waiting period between experiments is deliberately shortened so as to be comparable with some of the spin–lattice relaxation times under investigation; it therefore involves steady-state conditions. The danger with this technique is that pulse imperfections may have cumulative effects in the steady-state regime, introducing systematic errors in the observed T_1 values (*17*). For this application both the 180 and 90° pulses would need to be compensated for pulse imperfections.

Other applications which require accurate 180° pulses are to be found in the field of two-dimensional Fourier transform NMR spectroscopy. One such experiment generates spin echoes modulated by heteronuclear spin coupling by applying 180° pulses to the coupled heteronucleus (*18*). If these 180° pulses are imperfect then spurious responses appear in the two-dimensional spectrum. A similar problem arises in two-dimensional Fourier transform experiments designed to correlate the chemical shifts of two nuclear species, for example, protons and carbon-13 (*19, 20*); artifacts appear in the spectra if the 180° pulses used for "decoupling" are imperfect. There is a related experiment in conventional one-dimensional NMR where 180° pulses are used to flip the spin states of protons and thus effectively decouple or scale down the splittings in the carbon-13 spectrum (*21*). In this application the effects of pulse imperfections are cumulative, making compensation particularly important.

APPENDIX

Symmetry Properties of an $\alpha(X)$, $\beta(Y)$, $\alpha(X)$ Composite Pulse

The trajectories and final positions of nuclear magnetization vectors under the influence of a three-pulse sequence may be analyzed by examination of the three rotation matrices. During a pulse, an off-resonance isochromat is rotated through an angle α about a vector $\mathbf{r}$ tilted away from the XY plane by an angle θ given by Eq. [2]. The flip angle α is given by $\gamma H_{\text{eff}} t_p$, where H_{eff} is defined by Eq. [1]. Then the normalized rotation vector is

$$\mathbf{r}_X = (K, 0, S) \qquad [4]$$

for pulses about the X axis, and

$$\mathbf{r}_Y = (0, K, S) \qquad [5]$$

for pulses about the Y axis, where

$$K = H_1/H_{\text{eff}} \qquad [6]$$

and

$$S = \Delta H/H_{\text{eff}}. \qquad [7]$$

Rotation operators are then formed by straightforward vector algebra. For a pulse applied about the X axis,

$$\hat{R}_X(\alpha) = \begin{pmatrix} K^2(1-\cos\alpha)+\cos\alpha & S\sin\alpha & K(1-\cos\alpha)S \\ -S\sin\alpha & \cos\alpha & K\sin\alpha \\ K(1-\cos\alpha)S & -K\sin\alpha & S^2(1-\cos\alpha)+\cos\alpha \end{pmatrix} \qquad [8]$$

and where H_1 is applied along the Y axis,

$$\hat{R}_Y(\alpha) = \begin{pmatrix} \cos\alpha & S\sin\alpha & -K\sin\alpha \\ -S\sin\alpha & K^2(1-\cos\alpha)+\cos\alpha & K(1-\cos\alpha)S \\ K\sin\alpha & K(1-\cos\alpha)S & K^2(1-\cos\alpha)+\cos\alpha \end{pmatrix}. \qquad [9]$$

Each element possesses a symmetry with respect to the off-resonance parameter determined by the effect of changing the sign of S. For example, the element R_X^{31} clearly changes sign as S changes sign, and is thus antisymmetric, denoted $\bar{R}_X^{31}$.

The effect of a composite pulse $\alpha(X)$, $\beta(Y)$, $\alpha(X)$ on a unit magnetization vector $\mathbf{k}$ (initially along the Z axis) can now be calculated. The effect of the first pulse can be written

$$\hat{R}_{X1}k = \begin{pmatrix} R_{X1}^{13} \\ \bar{R}_{X1}^{23} \\ R_{X1}^{33} \end{pmatrix}. \qquad [10]$$

Application of the second pulse gives

$$\hat{R}_Y\hat{R}_{X1}k = \begin{pmatrix} R_Y^{11}\bar{R}_{X1}^{13} + \bar{R}_Y^{12}R_{X1}^{23} + R_Y^{13}R_{X1}^{33} \\ \bar{R}_Y^{21}\bar{R}_{X1}^{13} + R_Y^{22}R_{X1}^{23} + \bar{R}_Y^{23}R_{X1}^{33} \\ R_Y^{31}\bar{R}_{X1}^{13} + \bar{R}_Y^{32}R_{X1}^{23} + R_Y^{33}R_{X1}^{33} \end{pmatrix}. \qquad [11]$$

From Eq. [10] it is possible to see that in general the position of a magnetization vector at this point is completely asymmetric in the off-resonance parameter, each component consisting of a mixture of symmetric and antisymmetric terms. Nevertheless, under certain conditions, the application of a third pulse can restore symmetry to the final Z component. This third pulse, $\hat{R}_{X2}$, operating on the vector of Eq. [11] gives for the final Z component

$$\begin{aligned} M_Z = {} & \bar{R}_{X2}^{31}(R_Y^{11}\bar{R}_{X1}^{13} + \bar{R}_Y^{12}R_{X1}^{23} + R_Y^{13}R_{X1}^{33}) \\ & + R_{X2}^{32}(\bar{R}_Y^{21}\bar{R}_{X1}^{13} + R_Y^{22}R_{X1}^{23} + \bar{R}_Y^{23}R_{X1}^{33}) \\ & + R_{X2}^{33}(R_Y^{31}\bar{R}_{X1}^{13} + \bar{R}_Y^{32}R_{X1}^{23} + R_Y^{33}R_{X1}^{33}). \end{aligned} \qquad [12]$$

The terms $M_Z(a)$ which are antisymmetric in S thus become

$$M_Z(a) = \bar{R}^{31}_{X2} R^{11}_{Y} R^{33}_{X1} + R^{32}_{X2} \bar{R}^{23}_{Y} R^{33}_{X1} + R^{33}_{X2} R^{31}_{Y} \bar{R}^{13}_{X1} + R^{33}_{X2} \bar{R}^{32}_{Y} R^{23}_{X1}. \quad [13]$$

Examination of the form of the matrices [8] and [9] reveals that $M_Z(a)$ vanishes identically if the first and third pulses are identical. Under these conditions the resultant Z magnetization contains only terms in $M_Z(s)$ which are unchanged on changing the sign of S. Hence the contour maps drawn above are symmetrical with respect to positive and negative offsets ΔH. On the other hand, it is easy to show that the X and Y components display no such symmetry. Moreover the symmetry of the Z components is destroyed if the third pulse is applied along the $-X$ axis (simulated by interchanging $-K$ for K in Eq. [8]).

These symmetry properties of M_Z are important because they permit a doubling of the effective range of allowed transmitter offsets when a quadrature detection scheme is employed for signal detection. The analysis is useful in that it allows a certain insight into the properties of pulse sequences without explicit multiplication of many large rotation matrices. Beyond this, where exact knowledge of the trajectories of the magnetization vectors is required, computer simulation becomes a practical necessity.

ACKNOWLEDGMENTS

This work was made possible by an equipment grant and research studentships (S.P.K. and M.H.L.) from the Science Research Council.

REFERENCES

1. H. Y. Carr and E. M. Purcell, *Phys. Rev.* **94,** 630 (1954).
2. J. L. Markley, W. J. Horsley and M. P. Klein, *J. Chem. Phys.* **55,** 3604 (1971).
3. R. Freeman and H. D. W. Hill, *J. Chem. Phys.* **54,** 3367 (1971).
4. A. G. Redfield, *Phys. Rev.* **98,** 1787 (1955).
5. I. Solomon, *Compt. Rend.* **248,** 92 (1959).
6. I. Solomon, *Compt. Rend.* **249,** 1631 (1959).
7. H. C. Torrey, *Phys. Rev.* **76,** 1059 (1949).
8. S. Meiboom and D. Gill, *Rev. Sci. Instrum.* **29,** 688 (1958).
9. R. Freeman and S. Wittekoek, *J. Magn. Reson.* **1,** 238 (1969).
10. M. H. Levitt and R. Freeman, *J. Magn. Reson.* **33,** 473 (1979).
11. D. E. Demco, P. van Hecke, and J. S. Waugh, *J. Magn. Reson.* **16,** 467 (1974).
12. G. Bodenhausen, R. Freeman, G. A. Morris, R. Niedermeyer, and D. L. Turner, *J. Magn. Reson.* **25,** 559 (1977).
13. A. G. Redfield, 17th Experimental N.M.R. Conference, Pittsburgh, Pa., April 1976.
14. J. S. Waugh, L. M. Huber, and U. Haeberlen, *Phys. Rev. Lett.* **20,** 180 (1968).
15. R. Freeman and H. D. W. Hill, "Dynamic N.M.R. Spectroscopy" (F. A. Cotton and L. M. Jackman, Ed.), Chap. 5, Academic Press, New York, 1975.
16. D. Canet, G. C. Levy, and I. R. Peat, *J. Magn. Reson.* **18,** 199 (1975).
17. H. Hanssum, W. Maurer, and H. Ruterjans, *J. Magn. Reson.* **31,** 231 (1978).
18. G. Bodenhausen, R. Freeman, G. A. Morris, and D. L. Turner, *J. Magn. Reson.* **28,** 17 (1977).
19. A. A. Maudsley, A. Kumar, and R. R. Ernst, *J. Magn. Reson.* **28,** 463 (1977).
20. G. Bodenhausen and R. Freeman, *J. Magn. Reson.* **28,** 471 (1977).
21. R. Freeman, S. P. Kempsell, and M. H. Levitt, *J. Magn. Reson.* **35,** 447 (1979).